

# SINGLE-SHOT SPECTRAL ANALYSIS OF SYNCHROTRON RADIATION IN THE THz REGIME AT ANKA

A. Schmid\*, M. Brosi, E. Bründermann, K. Ilin, B. Kehrer, A. Kuzmin A.-S. Müller, J. Raasch, P. Schönfeldt, M. Schuh, M. Siegel, J. L. Steinmann, S. Wuensch, Karlsruhe Institute of Technology, Karlsruhe, Germany  
S. A. Kuznetsov, Novosibirsk State University, Novosibirsk, Russian Federation

## Abstract

Micro-bunching instabilities limit the longitudinal compression of bunches in an electron storage ring. They create substructures on the bunch profile of some hundred micrometer size leading to coherently emitted synchrotron radiation in the THz range. To detect the changing THz spectrum, single-shot bunch-by-bunch and turn-by-turn measurements are necessary. We present recent experiments at ANKA where the spectral information is extracted by simultaneous detection with several narrowband THz detectors, each of them sensitive in a different frequency range.

## INTRODUCTION

Coherent synchrotron radiation (CSR) in a synchrotron radiation facility can be created by reducing the bunch length. Above a certain electron density threshold, micro-bunching instabilities occur where the wakefield of the bunch acting back on itself in a bending magnet is stronger than the damping. This leads to a charge-density modulation on the bunch shape and to the formation of micro-structures. Due to coherence effects, these structures emit increased synchrotron radiation power in the terahertz regime. The time evolution of the micro-structures in longitudinal phase space therefore leads to strong fluctuations in the emitted CSR, the so-called "bursts" of THz radiation.

Figure 1 shows spectra calculated from a single-shot EOSD [1] measurement of the longitudinal bunch profile during a burst. The actual coherent enhancement is dependent on the number of particles in the bunch. Lower frequencies are shielded by the vacuum chamber cutoff, calculated by the parallel plates model [2]. For comparison, the calculated spectra of stable Gaussian-shaped bunches are shown for different rms bunch lengths. The micro-structures during the burst lead to an increased THz-intensity of several orders of magnitude, depending on the number of particles inside the bunch, compared to the Gaussian-shaped bunches.

Due to particle motion, the bunch shape changes continuously from turn to turn. Consequently the form-factor and the emitted spectrum vary accordingly. With a turn-by-turn analysis of the emitted THz radiation, information on the bunch profile can be gained. Based on superconducting  $\text{YBa}_2\text{C}_3\text{O}_{7-x}$  (YBCO) detector elements a multi-channel detector array is in development. This integrated planar detector array combines the fast response times of YBCO [3] with a narrowband spectral response of the individual array

\* alexander.schmid@kit.edu

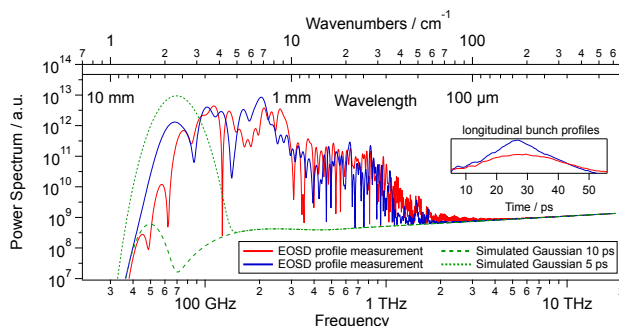


Figure 1: Calculated synchrotron radiation spectrum with vacuum chamber shielding low frequencies. The solid lines are bunch profile measurements done by EOSD and their calculated spectrum. The microstructures created by micro-bunching instability lead to an increase of THz radiation compared to a stable Gaussian shaped bunch (dashed lines).

elements, thus being well suited for the turn-by-turn analysis of the emitted spectrum of the synchrotron radiation. The final system will consist of four detectors coupled to narrowband antennas for frequencies from 140 GHz to 1 THz. Here we will present the design of a intermediate stage two-channel detector system for 140 GHz and 350 GHz along with first measurements at the ANKA storage ring.

## DETECTOR SYSTEM WITH INTEGRATED PLANAR YBCO ARRAY

The developed detector system consists of two main parts. Firstly, a liquid nitrogen bath cryostat with broadband readout lines and room-temperature electronics, and secondly a detector block holding the actual detector array. The room-temperature electronics is composed of broadband bias-tees and precision current sources used to supply the detectors with a current. Broadband amplifiers can be added if a higher signal level for the application is needed. The broadband readout design is optimized for frequencies up to 65 GHz with the goal not to deteriorate the fast intrinsic response times of the YBCO detectors.

The main part of the detector system is the integrated detector array. The individual array elements contain a sub- $\mu\text{m}$  sized superconducting detector bridge, embedded into double-slot antennas of different sizes in order to achieve the narrowband frequency response and needed frequency selectivity for spectroscopic measurements. The array design is shown in Fig. 2a. Four antennas are placed on a  $3 \times 3 \text{ mm}^2$  substrate of R-plane sapphire.

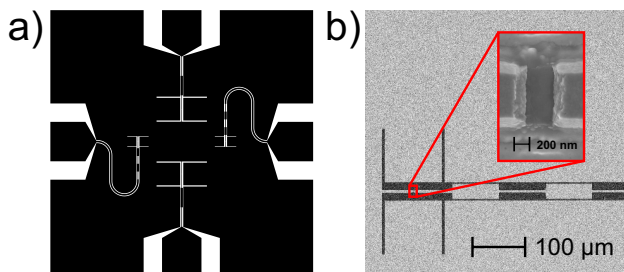


Figure 2: Integrated planar array of double-slot antenna-coupled YBCO detectors. a) Full view of the  $3 \times 3 \text{ mm}^2$  array with two antennas for 140 GHz and 350 GHz and broadband coplanar readout lines. b) SEM image of an antenna for 350 GHz and magnified view of the sub- $\mu\text{m}$  sized YBCO detector bridge (inset).

Thin YBCO films are deposited on top of the sapphire substrate using pulsed laser deposition. Epitaxial growth is enabled by the use of  $\text{CeO}_2$  and  $\text{PrBa}_2\text{Cu}_3\text{O}_{7-x}$  buffer layers. YBCO films as thin as 25 nm with critical temperatures of about  $T_c \approx 86 \text{ K}$  [4] can be deposited ensuring the operation of the YBCO detectors at liquid nitrogen temperatures. The deposition process also includes the in-situ sputtering of a thin gold film providing the metallization needed for the narrowband antennas and the RF readout lines.

A specially designed etching process for the actual YBCO detecting element combining argon-ion milling with wet-chemical etching of gold enables the patterning of sub- $\mu\text{m}$  feature sizes while preserving good electrical properties of the superconductor. Typical detector dimensions are in the range of a few 100 nm only, see inset in Figure 2b). Further details on the detector fabrication can be found in [5].

In order to maximize yield for the two channel detector system at the stage of detector preparation, two antennas on each array are optimized for the design frequencies of 140 GHz and 350 GHz, respectively. The two unused elements were shorted to ground while performing the measurements. The double-slot design (Fig. 2b) has been chosen due to its good coupling to Gaussian beams [6]. The combination with an immersion lens forms an integrated lens antenna.

The design of the antennas and the array has been optimized by simulations (with CST Microwave Studio©). Figure 3 shows the simulated reflection coefficient  $|S_{11}|$  for the two antenna design frequencies used in the array after the optimization procedure. Both designs show best matching and thus minimum reflection of received power at the intended design frequencies in combination with a narrowband behavior.

With regard to the placement of the individual elements in the array the main goal in this application is to achieve a level of sufficiently low mutual coupling between elements [7]. Otherwise, the crosstalk due to the mutual coupling will deteriorate the narrowband behavior of the antenna-detector combination. The array spacing was consequently also optimized to ensure that the spectral range of each detector is properly defined. Also, resonant low-pass filters were added

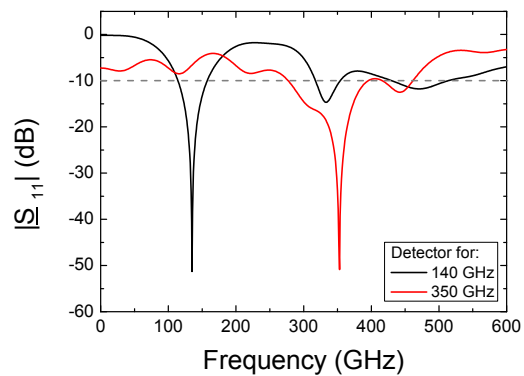


Figure 3: Simulated reflection coefficient  $|S_{11}|$  of the double-slot antennas in array configuration for a real antenna impedance of 150 Ohm. Both antennas show the expected narrowband behavior and good matching at their intended design frequency.

in the coplanar readout lines to decouple the detectors from the readout circuit for the design frequencies of the antennas (see Fig. 2b).

## MEASUREMENTS

The two-channel detector system with the integrated planar array has been tested at the IR2-Beamline [8] at ANKA with a single-bunch filling pattern in an operation mode with reduced bunch lengths [9]. The cryostat was placed in front of the diagnostic port and both detectors were read out simultaneously with a 32 GHz real-time oscilloscope (Agilent DSA-X 93204A).

Figure 4 shows the measured single-shot pulse signal for the two detectors. A delay is visible for the two signals with respect to each other because of differences in the length of the readout paths. The fast response time of the YBCO detectors is clearly visible with a full-width-half-maximum (FWHM) of 30.5 ps for the detector at 140 GHz and 33.6 ps for the 350 GHz detector. The response time is limited by the readout bandwidth and could be improved with a higher-bandwidth oscilloscope and an optimized design for the coplanar readout circuit.

In order to check the spectral response of the two detectors, a series of five THz bandpass-filters with different center frequencies from 140 GHz to 480 GHz were introduced into the optical path between the window of the beamline and the cryostat window of the detector system. The bandpass filters were implemented on the basis of multi-layer frequency selective surfaces produced with electroplating technology [10, 11] and were designed to provide a filtration bandwidth of around 20 % (FWHM) referred to the center frequency. The transmission behaviour of the used filters is shown in Fig. 5.

The averaged detector voltage behind the filters is given in Fig. 6. The detector for 140 GHz has maximum output voltage for the filter with 140 GHz center frequency and with increasing filter frequency the output voltage decreases.

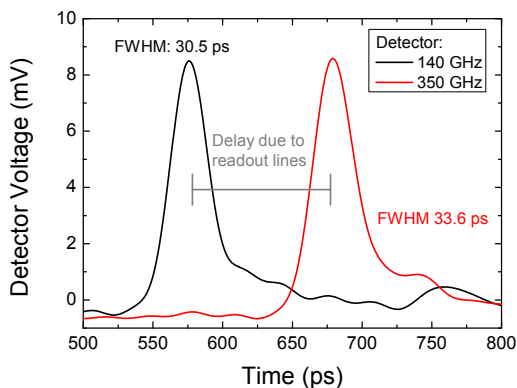


Figure 4: Measurement of the pulse shape of a single bunch of the synchrotron with simultaneous readout of two detectors of the array. The detectors show a fast response time of approx 30 ps limited by the readout bandwidth. The delay between both signals is due to different lengths of the readout cables.

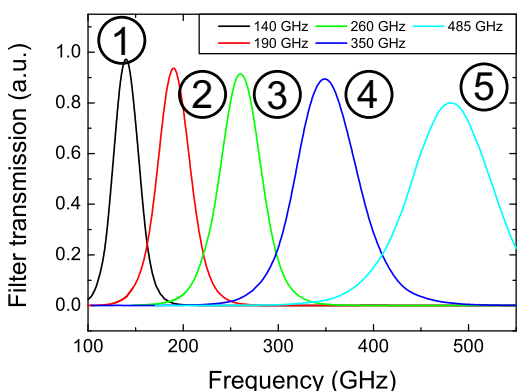


Figure 5: FTIR transmission measurement of used THz bandpass filters

The maximum output voltage of the 350 GHz detector is measured at higher bandpass filter frequency of 240 GHz. This reveals a clear difference in the spectral response of the two detectors. However, the results for the two detectors have not been normalized to the spectrum of the synchrotron radiation (compare Fig. 1) which might explain the fact that the highest output is not seen at the detectors design frequency.

### SUMMARY AND OUTLOOK

We have presented the design and first measurements of our current YBCO detector array for two frequencies. Improvements in the optical setup of the detection system and a larger number of narrowband detectors sensitive at higher frequencies are promising next steps towards an improved single-shot THz-spectroscopy system. Currently a detector system with four array-elements is in the final stages of development. Together with the KAPTURE [12] readout electronics this detector system allows the simultaneous detection of spectral THz information as well as longitudinal

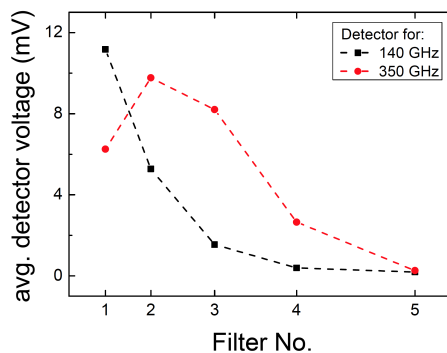


Figure 6: Averaged measurement of the detector output voltage with THz bandpass filters in the optical path of the detector system. The measurement is not normalized to the spectrum of the synchrotron. The response of the 350 GHz detector is visibly shifted to higher frequencies compared to the 140 GHz detector.

and transverse bunch signals at ANKA [13] to improve the observation of micro-bunching instabilities.

### ACKNOWLEDGMENTS

We would like to thank Y.-L. Mathis and his team from the ANKA Infrared-Group for support during the beam-time. This work was supported in part by the Helmholtz International Research School for Teratronics (HIRST), the Karlsruhe School of Elementary Particle and Astroparticle Physics: Science and Technology (KSETA), BMBF contract number 05K13VK4 and the Ministry of Education and Science of the Russian Federation (State Assignment Contract No. 3002).

### REFERENCES

- [1] N. Hiller *et al.* in *Proc. IPAC 14*, pp. 1909-11.
- [2] A. Novokhatski, *ICFA Beam Dyn. Newsl.* **57**, 127-144 (2012).
- [3] P. Thoma *et al.*, *Appl. Phys. Lett.* **101**, 142601 (2012).
- [4] P. Probst *et al.*, *Phys. Rev. B* **85**, 174511 (2012).
- [5] P. Thoma *et al.*, *IEEE Trans. Appl. Supercond.* **23**, 3 (2013).
- [6] D. Filipovic *et al.*, *IEEE Trans. Microw. Theory Techn.* **41**, 10 (1993).
- [7] A. Schmid *et al.*, "Integrated Four-Pixel Narrowband Antenna Array for picosecond THz Spectroscopy", *IEEE Trans. Appl. Supercond.*, to be published.
- [8] Y.-L. Mathis *et al.*, *J. Biol. Phys.*, **29**, 313-318 (2003).
- [9] A.-S. Müller *et al.*, *ICFA Beam Dynamic Newsletter* **57**, 154-165 (2012).
- [10] M.K.A. Thumm *et al.*, *Terahertz Sci. Tech.*, Vol.5 No.1, pp. 18-39 (2012).
- [11] S.A. Kuznetsov *et al.*, in *Proc. of 44th EuMC*, pp. 881-884 (2014).
- [12] C.M. Caselle *et al.*, in *Proc. of IPAC'14*, pp. 3497-9.
- [13] B. Kehrer *et al.*, presented at IPAC'16, Busan, Korea, May 2016, paper MOPMB014.